Advances in Science and Technology Research Journal

*Advances in Science and Technology Research Journal* 2023, 17(5), 130–139
https://doi.org/10.12913/22998624/171490
ISSN 2299-8624, License CC-BY 4.0

Received: 2023.07.10
Accepted: 2023.08.23
Published: 2023.10.20

# Fracture Surface Topography Parameters for S235JR Steel Adhesive Joints after Fatigue Shear Testing

Andrzej Kubit[1*], Wojciech Macek[2], Władysław Zielecki[3], Paulina Szawara[4], Mariusz Kłonica[5]

[1] Department of Manufacturing and Production Engineering, Rzeszow University of Technology, al. Powst. Warszawy 8, 35-959 Rzeszów, Poland

[2] Faculty of Mechanical Engineering and Ship Technology, Gdańsk University of Technology, ul. Gabriela Narutowicza 11/12, 80-233 Gdańsk, Poland

[3] Department of Manufacturing and Production Engineering, Rzeszow University of Technology, al. Powst. Warszawy 8, 35-959 Rzeszów, Poland

[5] Department of Materials Forming and Processing, Rzeszow University of Technology, al. Powst. Warszawy 8, 35-959 Rzeszów, Poland

[5] Lublin University of Technology, ul. Nadbystrzycka 38D, 20-618 Lublin, Poland

* Corresponding authors' e-mail: akubit@prz.edu.pl

## ABSTRACT

This paper presents the experimental results of a study investigating the effect of holes and notches made on the overlap ends on the strength of adhesive joints. Single-lap joints made of S235JR steel sheets bonded with Araldite 2024-2 epoxy adhesive were tested. For comparative reasons, static shear strength tests and high-cycle fatigue strength tests were performed. Adhesive-filled joints having three holes, each with a diameter of 3 mm, and notches, each 3 mm wide and 4 mm long, were tested and compared with reference joints, i.e. without modification. The assumption was to determine whether the structural modifications would reduce the peak peel and shear stresses that are typical of this type of joints. Results of the static strength tests showed no significant effect of the applied modifications on the strength of the joints. However, in terms of fatigue strength, the results demonstrated a significant improvement in fatigue life, the value of which increased in the low-cycle fatigue region by 328.6% for the joint with notches and by 640.8% for the joint with holes. A smaller yet still positive effect of the applied modifications was shown for high-cycle fatigue. For a variable load with the maximum value of 9 MPa, the fatigue life increased by 215.9% for the variant with notches and by 183.3% for the variant with holes. Surface topography of fatigue fractures was examined by determining roughness parameters on the overlap ends in the samples. Significant differences were shown, with the selected roughness parameters being significantly lower for the reference variant than for the variants with notches and holes. It was shown that the applied structural modifications led to increasing the fatigue strength to 8.5 MPa for the limit number of cycles equal to 2·106, when compared to the reference variant for which the fatigue strength was 8 MPa.

**Keywords:** adhesive joints, surface topography parameters, fatigue shear tests.

## INTRODUCTION

In recent years, structural adhesive joints have become more and more widely used to produce lightweight and high-strength structures. Adhesive joints are widely used in the construction of means of transportation, especially in the automotive, aviation and railway industry, because they enable joining materials with different properties, which is an extremely important feature of modern designs [1]. Adhesive joints are used not only in the construction of new structures, but

they are also used to repair e.g. aviation structures [1]. The strength of adhesive joints depends on many factors, such as adherend surface preparation method, bonding process conditions and adherend geometry [2–6].

A general recommendation regarding the design of adhesive joints and their shape is to make shear stresses dominate. In reality, however, pure shear hardly ever occurs in lap joints._Instead, there occurs a complex state of stress, one in which normal stresses causing undesirable peeling also play an important role [7]. On the overlap end of the loaded joint, there occurs a stress concentration [7] that usually initiates joint failure.

Due to the increasing use of adhesive joints in structures, there is a need for research aimed at providing high-strength reliable joints. In the literature of the subject one can find many solutions for strengthening adhesive joints. Generally, these techniques can be divided into two main groups. The first group includes methods for increasing adhesive joint strength by modifying adhesives in order to improve their mechanical properties and adhesion. Wernik et. al. [8, 9] investigated the problem of modifying structural epoxy adhesives through the use of nanofillers in the form of carbon nanotubes. Gkikas et. al. [10] studied the possibility of improving the parameters of adhesive joints via the use of nanofillers, e.g. ceramic materials.

The other group comprises techniques relating to adherend geometry modification aimed at reducing peel and shear stress peaks which usually occur on the overlap end of the joint [11, 12]. A frequently used way of reducing stress in joints is adherend bevelling [13–15]. Both internal tapers in adherends are used, which leads to a local increase in the adhesive layer thickness [16]. Another method for achieving uniform stress distribution is the use of external tapers that do not affect the thickness of the adhesive layer, but cause a local reduction in the stiffness on the overlap end [17]. In addition to tapering, fillets on overlap ends are also successfully used [18, 19]. The effectiveness of these simple modifications was proved not only by numerous experimental studies [16, 20, 21], but also by The Finite Element Method (FEM) numerical analyses [22–25]. This problem has been focused on in numerous studies investigating the effect of various taper sizes on stress reduction, e.g. in a study by Belingardi et al [24]. Fessel et al. [26] proposed another method of peak stress reduction in joints by changing joint geometry. Joints with wavy geometry were tested, and the results showed a significant increase in their strength. At the same time, it was showed that such modifications of joint geometry made it possible to reduce the peak peel and shear stresses in the range of 8 to 40% compared to the flat geometry adherends. Campilho et al. [27] investigated the possibility of stress reduction in the joint by using deflected adherends in the lap joint. It was found that the proposed solution made it possible to reduce peel stresses in the joint.

Sancaktar and Simmons [28] studied the effect of notches made in adherends on the properties of aluminium alloy adhesive lap joints. Using FEM, they showed that it was possible to reduce the normal stress peak on the overlap end by 60%. However, the experimental results showed an 8% increase in the static shear strength. Similar analyses using FEM were conducted by Yan et. al. [29]. They considered in detail different sizes of notches made on the overlap ends, showing the possibility of significant reduction in the peak peel and shear stresses.

This paper presents the experimental results of a study investigating the influence of notches and holes made on the overlap ends on the strength properties of single-lap adhesive joints. Static shear strength tests as well as fatigue strength tests were carried out. For fatigue fractures, a surface topography analysis was performed, showing differences in fatigue cracking mechanisms. The development of surface metrology opens up new possibilities for investigating surface features in many engineering areas and evaluating surface characteristics. Experimental characterization of surface textures produced as a result of quasi-static and cyclic loading is fundamental to determine their suitability for different applications as well as to investigate load histories and adhesive joint effects.

The issue discussed in the work is important because a significant impact on improving the fatigue lifetime of joints has been demonstrated through the use of modifications that are relatively simple from a technological and economic point of view. Nowadays, striving to minimize the weight of the construction of means of transport, every issue that allows to improve the strength properties without increasing the weight is important. In the literature there are many research results determining the effect of beveling and rounding the edges of adherends on the strength of adhesive joints. These are the results of both experimental

research and FEM analysis. However, there are no studies in the literature considering the effect of notches and holes on the fatigue properties of joints. Therefore, the issue presented in the work should be considered as new and original. In addition, the method of analyzing fatigue fractures based on a comparative analysis of the fracture surface topography should also be considered as an original approach.

## MATERIALS AND METHODS

Static and fatigue shear tests of adhesive joints were carried out on samples the dimensions of which are shown in Figure 1. Both adherends were made of S235JR steel. Surface preparation before adhesive joining involved sandblasting with alumina corundum F40. The sandblasting process was conducted with the following parameters: air pressure 0.8 MPa, nozzle-to-sample distance 150 mm, blasting time 60 s. Prior to bonding, the surfaces of the samples were cleaned with acetone. The samples were bonded with the Araldite 2024-2 epoxy adhesive (supplied by Huntsman Corporation, Texas, USA). The adhesive-bonded samples were then cured under a constant pressure of 0.1 MPa at room temperature for 24 hours.

Three different variants of samples were prepared and then tested. The tests were aimed at determining the impact of simple structural changes on the static and fatigue properties of the joints. Figure 2 shows the tested variants of joints. The base variant had no modifications and was considered as the reference (Fig. 2a), the variant with holes had three holes, each with a diameter of 3 mm and a spacing of 6.5 mm, which were made on the overlap end, while the variant with notches had three notches made on the overlap end, each notch being 3 mm wide and 4 mm long (Fig. 2c). In the variants with modifications, both holes and notches were filled with the adhesive.

Static strength tests were carried out using the Zwick/Roell Z-100 universal testing machine. The test speed was 5 mm/min, five repetitions were performed for each variant.

Fatigue tests were performed using the HT-9711 Dynamic Testing Machine (Hung Ta Instrument Co., Taichung City, Taiwan). As part of the fatigue tests, a sinusoidal waveform of the load with a frequency of 30 Hz was used, and the fatigue stress ratio was equal to R = 0.1. To determine fatigue curves for each variant, five load levels were used, each of which was repeated four times. When the number of cycles for a given sample significantly differed from the results for the other samples, such case was rejected and the measurement was repeated. The limit number of cycles was set to $2 \cdot 10^6$ in the study.

The surfaces of selected fatigue fractures were subjected to topography analysis in order to determine differences in fatigue mechanisms for the considered variants. Surface examination was made in the ROI using volume parameters *Vx* and height parameters *Sx*, as specified in the ISO 25178-2 standard [30]. As part of the analysis, two parameters were used: an arithmetic mean height *Sa* and a void volume *Vv*.

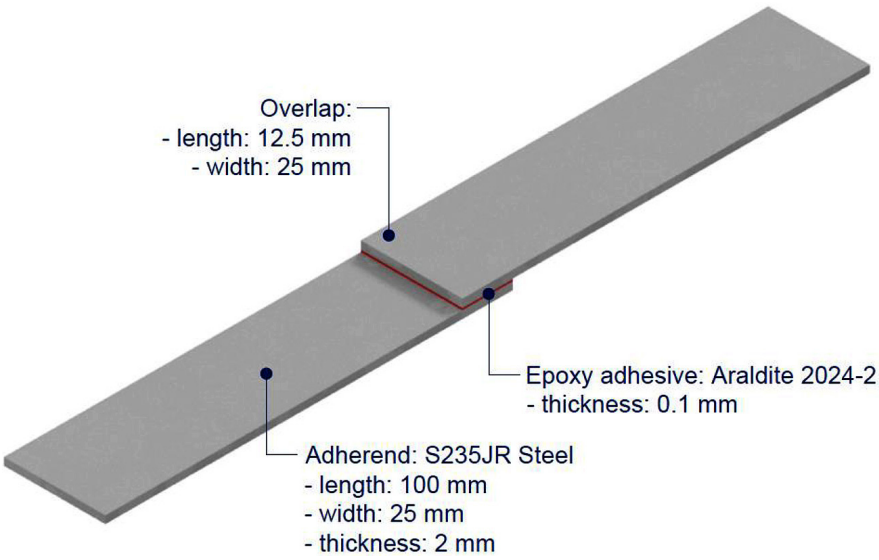


**Figure 1**. Geometry and dimensions of a lap-joint specimen for static and fatigue tensile/shear tests (units: mm)

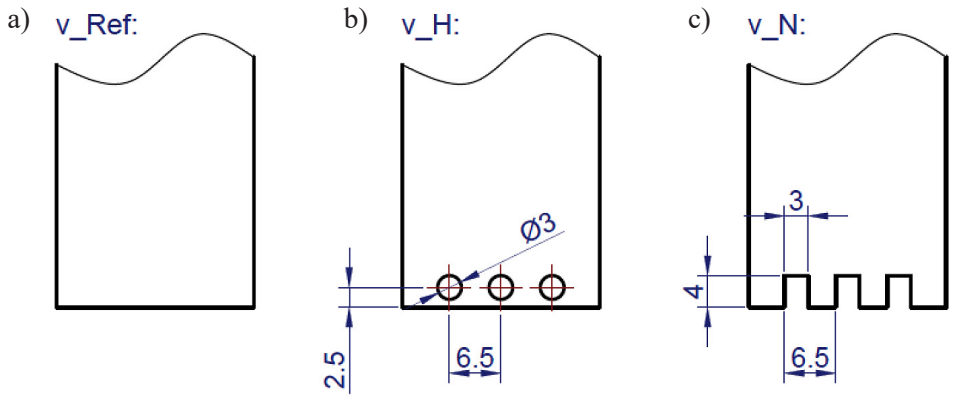


**Figure 2.** Geometry of tested adherends: reference variant (a), variant with holes (b) and variant with notches (c) (units: mm)

The examined surfaces were also analysed by calculating a fractal dimension $D_f$ [31]. With the fractal dimension $D_f$, as the surface is split, the algorithms have to process the number of iterations that occur. The resolution scale defines the number of repetitions. In this study, 96 points were used for extra-fine resolution. The morphological envelope method (MEM) captures the upper and lower envelopes which are then considered by morphological opening and closing, defining a composition component which assumes the form of a horizontal line segment with a length δ. The calculated surface volume ($V\delta$) is displayed through a relationship of $\ln(V\delta)/\ln(\delta)$. To estimate the value of $D_f$, a line is fitted using the least squares method (LSM). The slope of the fitted line calculated as an absolute value corresponds to $D_f$.

Another surface topography parameter considered in this study for fatigue fractures was texture isotropy [32]. The direction of the geometric structure of a given surface depends on the cause of fracture and results from the kinematics of the fracture process. The isotropy of a medium is generally based on the fact that it exhibits the same physical or geometric properties in all directions. The isotropy of a surface, therefore, means that the surface has the same structure in all directions. It is also a perfectly symmetrical structure with respect to all possible axes of symmetry. As part of these analyses, two parameters were used: arithmetic mean height, *Sa* and void volume, *Vv*. The examined surfaces were also analyzed by calculating the fractal dimension $D_f$ [33, 34].

## RESULTS AND DISCUSSION

Table 1 lists the average values of static shear strength of the joints for individual variants, as well as their standard deviations. For each variant, a cohesive failure was obtained, which proves that the surface preparation and the bonding process were correct. The results of the static strength tests indicate that the applied structural modification by making holes and notches on the overlap ends of the joined sheets do not have a significant impact on the properties of the joint. Still, there is a slight increase in the average strength of the joint for the variant with notches, its value being 24.38 MPa, when compared to the reference variant for which the average strength is 23.83 MPa. However, it should be noted that the variants with the structural modifications are characterized by significant differences of the results compared to the reference variant. On the overlap ends of the joined sheets, the standard deviation is equal to 3.145 MPa for the variant with holes and to 0.645 MPa for the reference variant. The greater difference in the strength results may be due to the fact that the notches and holes were not filled with the adhesive in a uniform manner for technological reasons. In addition, the adhesive filling

**Table 1.** Static strength test results of adhesive joints

| Variant | v_Ref | v_H | v_N |
|---|---|---|---|
| Shear strength (MPa) | 23.83 | 22.05 | 24.38 |
| Standard deviation (MPa) | 0.645 | 3.145 | 1.027 |

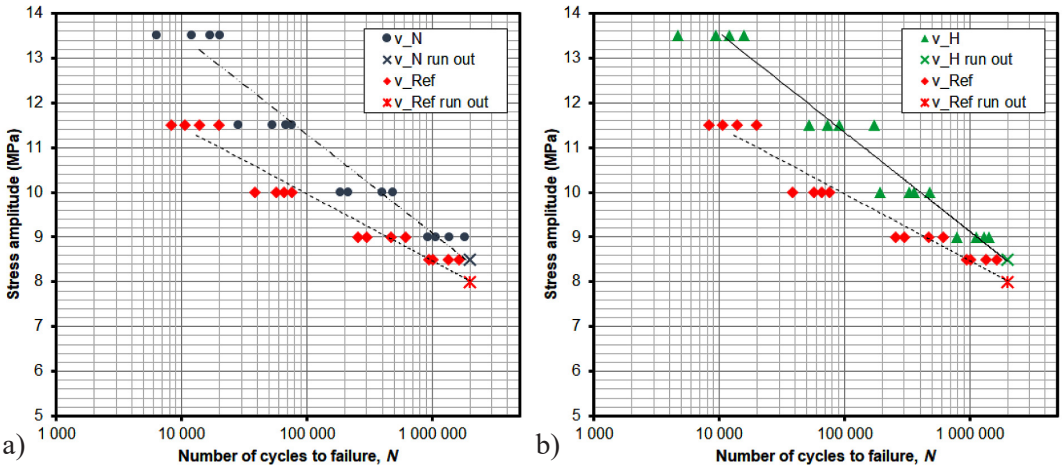


**Figure 3.** Comparison of S-N curves for the reference joint and joints with holes (a) and notches (b)

the notches and holes might have contained random defects such as air bubbles, which could also contribute to the differences in the results. The above-mentioned phenomena may be the cause of locally different mechanical properties of the joint, which translates into significant differences in the results obtained for individual samples.

As far fatigue strength test results are concerned, significant differences have been observed for the variants with the modifications. Fig. 3 shows the fatigue curves for the considered variants of joints. Fig. 3a shows the comparison of S-N curves for the reference variant and the variant with notches, while Fig. 3b shows the S-N curves obtained for the variant with holes and the reference variant. It can be observed that the applied structural modifications have a significant impact on the fatigue life of the samples. A particularly significant effect is shown for low-cycle fatigue. For a variable load of 11.5 MPa, the fatigue life of the reference variant is 13,168 cycles on average. For the same level of variable load, the fatigue life of the variant with notches is 56,437 cycles, which amounts to a significant increase of 328.6%. An even more favourable effect is observed for the variant with holes, for which the average fatigue life under a load of 11.5 MPa is 97,548 cycles, which amounts to a 640.8% increase compared to the reference variant.

With decreasing the load, the differences in fatigue life become smaller. By analysing the differences in this parameter for the high-cycle fatigue region, the average fatigue life is determined for a cyclic stress of 9 MPa. The reference variant has an average fatigue life of 410,516 cycles, while for the variant with notches the average fatigue life is 1,297,010 cycles, which amounts to a 215.9% increase. On the other hand, for the variant with holes, the fatigue life is 1,162,916 cycles, which is a 183.3% increase in relation to the reference variant.

For the assumed limit number of cycles equal to $2 \cdot 10^6$, the fatigue strength of the reference variant is 8 MPa, while for both variants with structural modifications its value is 8.5 MPa. This confirms that simple structural modifications can significantly contribute to the improvement of fatigue properties of structural adhesive joints. The positive impact of the applied structural modifications is proved by the local flexibility of the joint on the overlap end, i.e. in the area of high stress concentration.

Figures 4a-c show the macroscopic views of fragments of the fatigue fracture surfaces in selected samples of all considered variants. Regarding the reference variant, the sample selected for fractography analysis failed after 19,832 cycles and a load of 11.5 MPa. For the variant with holes, the fracture surface was taken from a sample which was loaded with the same level of cyclic stress and failed after 73,808 cycles. For the variant with notches, a sample that failed after 76,012 cycles under a maximum fatigue load value of 11.5 MPa was selected for fractographic analysis. As for the reference joint, the cracking is uniform in the examined area on a macroscopic scale. However, for the joints with notches and holes, the cracking mechanism is completely different. The adhesive-filled notches and holes are a region of greater elasticity because with each fatigue cycle, the entire volume of the adhesive is deformed in the hole/notch region, which means that the adhesive layer thickness is comparable to

the thickness of the joined sheets, i.e. 2 mm. On the other hand, in the reference joint, the thickness of the adhesive layer is only about 0.1 mm. The differences in the cracking mechanism indicate that the cyclic deformation of the adhesive filling the notches and holes absorbs a certain amount of energy and that this phenomenon prevents the propagation of fatigue cracks in the proper adhesive layer between the sheets.

To gain more insight into the differences between fatigue mechanisms of the considered joint variants, the surface topography of fatigue fractures was examined. Measurements of roughness parameters were made on the fragments of fatigue fracture surfaces marked in Figures 4a-c. Regarding the reference variant, the overlap end and adjacent regions spaced by 2 mm were analysed (Fig. 4a). For the variant with holes and notches, the regions near the central hole and notch and those spaced by 2 mm were selected for analysis, as marked in Figures 4b and 4c. Tables 2-4 list the roughness results for individual fragments of fatigue fractures. The greatest differences in the values of roughness parameters can be observed for the fracture area closest to the overlap end of the adhesive joint. As for the reference (Table 2), the roughness values are significantly lower than those obtained for the variants with modifications. The arithmetic mean height *Sa* of the reference variant is 4.44 µm, while for the variant with holes it is 56.35 µm in a similarly located fatigue fracture and 35.16 µm for the variant with notches. In the regions located further from the overlap end, no such great difference can be observed. However, the overlap end is the region where the most significant fatigue phenomena occur. Due to the characteristic stress concentration on the overlap ends, this is where fatigue

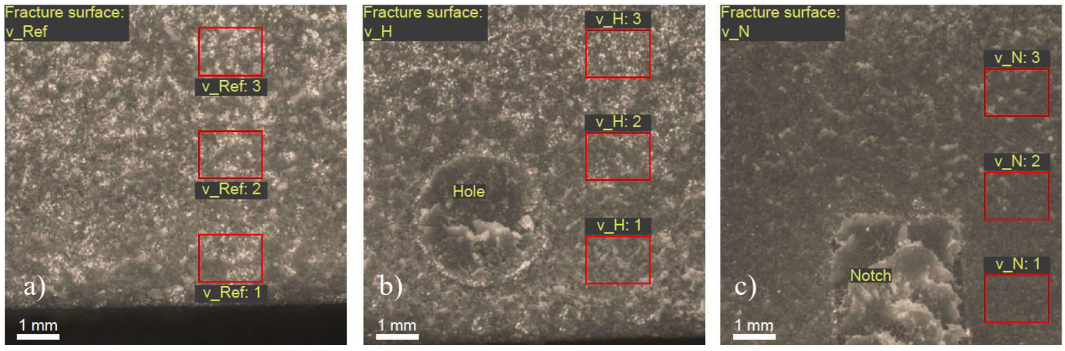


**Figure 4.** Macroscopic views of selected fatigue fractures with marking of roughness measurement areas for the following variants of samples: reference (a), with holes (b) and with notches (c)

**Table 2.** 3D surface topography in selected areas of fatigue fracture for the reference variant

| v_Ref: 1 | v_ Ref: 2 | v_ Ref: 3 |
|---|---|---|
| 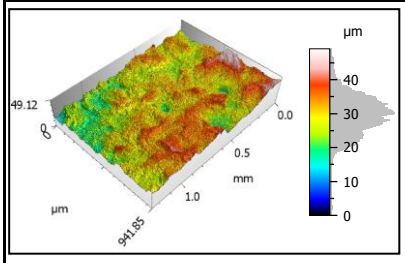 | 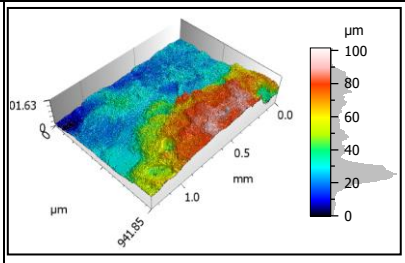 | 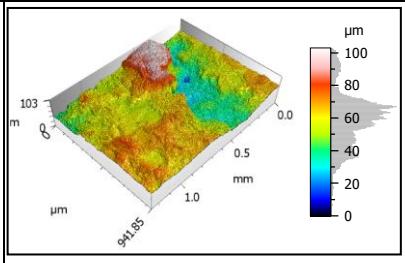 |
| *Sq* = 5.67 µm | *Sq* = 22.74 µm | *Sq* = 14.84 µm |
| *Ssk* = -0.24 | *Ssk* = 0.68 | *Ssk* = 0.21 |
| *Sku* = 4.36 | *Sku* = 2.07 | *Sku* = 3.22 |
| *Sp* = 19.37 µm | *Sp* = 59.38 µm | *Sp* = 43.97 µm |
| *Sv* = 29.75 µm | *Sv* = 42.25 µm | *Sv* = 59.03 µm |
| *Sz* = 49.12 µm | *Sz* = 101.63 µm | *Sz* = 103.00 µm |
| *Sa* = 4.44 µm | *Sa* = 19.82 µm | *Sa* = 11.50 µm |

**Table 3.** 3D surface topography in selected areas of fatigue fracture for the reference variant

| v_H: 1 | v_H: 2 | v_H: 3 |
|---|---|---|
| 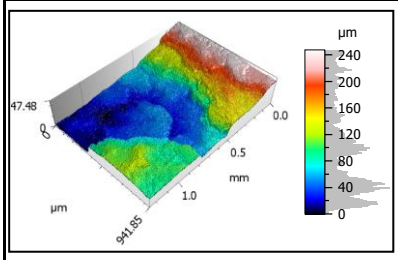 | 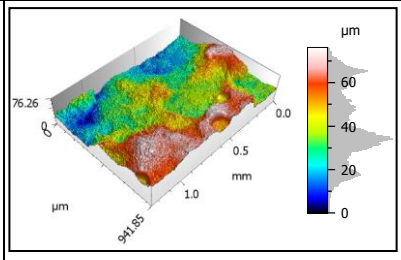 | 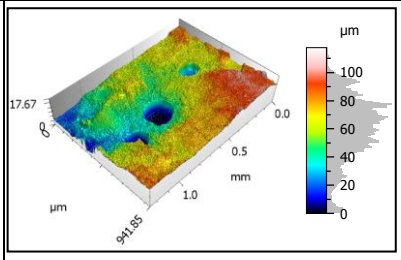 |
| *Sq* = 67.73 µm | *Sq* = 16.00 µm | *Sq* = 21.43 µm |
| *Ssk* = 0.69 | *Ssk* = 0.24 | *Ssk* = -0.55 |
| *Sku* = 2.33 | *Sku* = 2.10 | *Sku* = 3.06 |
| *Sp* = 152.21 µm | *Sp* = 36.03 µm | *Sp* = 56.57 µm |
| *Sv* = 95.26 µm | *Sv* = 40.23 µm | *Sv* = 61.10 µm |
| *Sz* = 247.48 µm | *Sz* = 76.26 µm | *Sz* = 117.67 µm |
| *Sa* = 56.35 µm | *Sa* = 13.43 µm | *Sa* = 17.05 µm |

**Table 4.** 3D surface topography in selected areas of fatigue fracture for the variant with notches

| v_N: 1 | v_N: 2 | v_N: 3 |
|---|---|---|
| 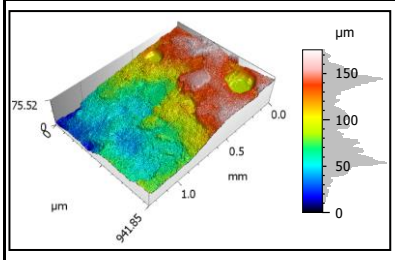 | 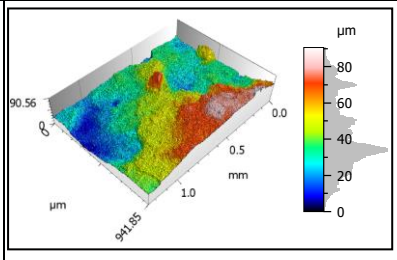 | 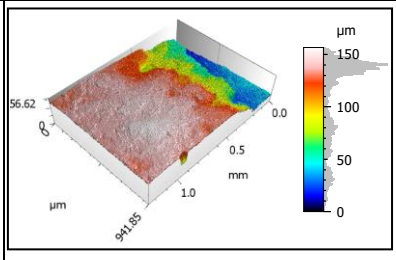 |
| *Sq* = 39.59 µm | *Sq* = 18.04 µm | *Sq* = 39.58 µm |
| *Ssk* = 0.14 | *Ssk* = 0.47 | *Ssk* = -1.00 |
| *Sku* = 1.68 | *Sku* = 2.40 | *Sku* = 2.62 |
| *Sp* = 79.88 µm | *Sp* = 48.75 µm | *Sp* = 45.70 µm |
| *Sv* = 95.63 µm | *Sv* = 41.82 µm | *Sv* = 110.92 µm |
| *Sz* = 175.52 µm | *Sz* = 90.56 µm | *Sz* = 156.62 µm |
| *Sa* = 35.16 µm | *Sa* = 14.86 µm | *Sa* = 34.12 µm |

cracking is initiated and propagates into the joint centre. Thus, the hypothesis is confirmed that the notches and holes filled with adhesive cause the accumulation of some energy associated with the deformation of the joint in each cycle. The more severe fatigue cracks on the fracture surface at the notches and at the openings prove that the propagation of fatigue cracks was inhibited in these regions, because the propagation process evidently absorbed more energy. Surface topography parameters were measured on the fragments of fatigue fractures marked in Figures 4a-c. Regarding the reference variant, the overlap end and adjacent regions spaced by 2 mm were analysed (Fig. 4a). For the variant with holes and notches, the regions near the central hole and notch and those spaced by 2 mm were selected for analysis, as marked in Figures 4b, c.

The local increase in elastic deformability in the region of notches and holes filled with the adhesive, which contributed to energy absorption, significantly affected the joint area between the notches and holes. As previously observed, this desired phenomenon was particularly noticeable in the region of low-cycle fatigue, which proves that the most significant fatigue phenomena occur

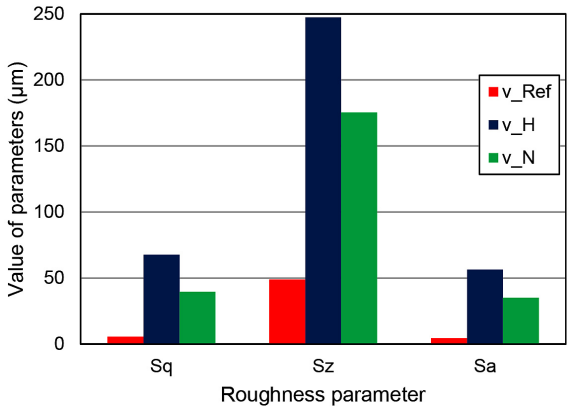


**Figure 5.** Comparison of selected roughness parameters of fatigue fractures of joints of all considered variants for the first measurement area

on the overlap ends in the joints. For lower values of alternating load responsible for high-cycle fatigue, the entire surface of the joint was more uniformly loaded, hence the lower impact of local flexing of the joint on the overlap ends. The significance of the phenomena occurring on the overlap ends is illustrated via selected roughness parameters. The significance of the phenomena occurring on the overlap ends is illustrated via selected roughness parameters plotted in Fig. 5. The figure also shows the values of the fractal dimension ($D_f$) to show, in contrast, that this surface parameter does not change significantly in the case of individual variants.

The most significant differences in the values of roughness parameters were shown for the first measurement area, i.e. the closest to the front edge of the joint. Therefore, for this area, a comparison of selected parameters for fatigue fractures of individual variants was made. The root-mean-square height of selected area (*Sq*) parameter for the variant with holes of 67.73 µm is almost 12 times greater than the corresponding parameter at the fatigue fracture surface of the reference joint (*Sq* = 5.67 µm). In the case of a joint with notches, this value is 7 times greater. Moving on to the maximum height of selected area (*Sz*), on the surface of the fatigue fracture of the joint with the holes, the value of this parameter increased by more than 5 times compared to the reference variant (*Sz* = 49.12 µm). Moving on to the variant with notches, a 3.5-fold increase in the Sz value was observed. The last of the parameters selected here showing significant variability in the comparative analysis is the average height of the selected area (*Sa*). For the variant with holes, the value of this parameter was *Sa* = 56.35 µm, which is almost 13 times higher than the reference joint (*Sa* = 4.44 µm). In turn, for the variant with notches, the considered parameter is almost 8 times higher than the reference case, as it is *Sa* = 35.16 µm.

It should be noted that the comparison was made for fatigue fractures, for which the average fatigue lifetime was 640.8% and 328.6% higher, respectively, for the variants with holes and notches than the fatigue lifetime of the reference joint. All variants were loaded with the same level of variable load (11.5 MPa), but the reference joint was failured in the low-cycle fatigue area. On the other hand, variants with modifications exceeded the low-cycle fatigue limit, hence it can be considered that they were subjected to mechanisms typical of high-cycle fatigue.

Comparative analysis of the fracture surfaces showed significant differences for individual joint variants, which proves that the adopted direction of research is correct. It was shown that the mechanism of fatigue cracking for the variants with the tested structural changes is different from the reference variant. As it has been shown by the measurements of fracture roughness parameters, in the areas adjacent to notches and holes, cracking has a different character than for the uniform surface of the reference joint. Notches and holes absorb a certain amount of energy with each alternating load cycle, which is confirmed by the demonstrated significant increase in fatigue lifetime. However, these are only preliminary studies aimed at determining the validity of the adopted methodology, they lack quantitative analysis, which outlines further research directions. As part of future work, a more detailed analysis is planned to determine more detailed relationships between individual roughness parameters and fatigue cracking mechanisms.

## CONCLUSIONS

Based on the results of the study aimed at determining the effect of notches and holes made on the overlap ends to reduce the peak peel and shear stresses, the following conclusions have been drawn. The use of notches and holes filled with the adhesive does not significantly affect the static shear strength of adhesive joints. Joints with such structural modifications are characterized by a greater scatter of strength results, which may be

due to uneven filling of notches and holes with the adhesive. In the low-cycle fatigue region, the tested modifications have a very significant impact on increasing the fatigue life of the samples. For a variable load of 11.5 MPa, the fatigue life increase amounted to 328.6% for the variant with notches and to 640.8% for the variant with holes in relation to the reference variant.

A smaller yet still positive effect of the applied modifications was shown for high-cycle fatigue. For a variable load with the maximum value of 9 MPa, the fatigue life increased by 215.9% for the variant with notches and by 183.3% for the variant with holes. Regarding low-cycle fatigue, it was observed that with each fatigue cycle, the stress peak on the overlap ends was reduced by the adhesive volume in notches and holes having lower stiffness than steel. For a lower live load value, this effect was smaller because the stresses in the joint were more uniform. It was shown that the applied structural modifications led to increasing the fatigue strength to 8.5 MPa for the limit number of cycles equal to $2 \cdot 10^6$, when compared to the reference variant for which the fatigue strength was 8 MPa. The analysis of the fatigue fracture surface demonstrated that on the overlap ends where fatigue cracking would initiate, the selected roughness parameters were much lower for the reference variant than those of the variants with notches and holes. This may indicate a higher cracking energy in the variants with modifications. Some part of the energy was dissipated by the adhesive volume in the notches and holes.

In further studies, the proposed methodology should be extended to investigate the entire fracture surface in elements with joints of different shapes, sizes and materials, as well as having different load histories in order to find a general formula for estimating the number of cycles to failure $N_f$ or the cause of damage.

## REFERENCES


1. da Silva L.F.M., das Neves P.J.C., Adams R.D., et al. Analytical models of adhesively bonded joints – Part I: literature survey. Int. J. Adhes. Adhes., 2009; 29: 319–330.
2. Kadioglu F., Adams R.D. Flexible adhesives for automotive application under impact loading. Int. J. Adhes. Adhes., 2015; 56: 73–78.
3. Davies P, Sohier L, Cognard J-Y, et al. Influence of adhesive bond line thickness on joint strength. Int. J. Adhes. Adhes., 2009; 29: 724–736.
4. Karachalios E.F., Adams R.D., da Silva L.F.M. The behaviour of single lap joints under bending loading. J. Adhes. Sci. Technol., 2013; 27: 1811–1827.
5. Bartczak B., Mucha J., Trzepieciński T. Stress distribution in adhesively-bonded joints and the loading capacity of hybrid joints of car body steels for the automotive industry. Int. J. Adhes. Adhes., 2013; 45: 42–52.
6. da Silva L.F.M., das Neves, P.J.C., Adams R.D., Spelt J.K. Analytical models of adhesively bonded joints part I: literature survey. Int. J. Adhesion Adhes., 2008.
7. Wernik JM, Meguid SA. Multiscale micromechanical modelling of the constitutive response of carbon nanotube-reinforced structural adhesives. Int J Solids Struct 2014; 51: 2575–89.
8. Wernik JM, Meguid SA. On the mechanical characterization of carbon nanotube reinforced epoxy adhesives. Mater Des 2014; 59: 19–32.
9. Gkikas G, Sioulas D, Lekatou A, Barkoula NM, Paipetis AS. Enhanced bonded aircraft repair using nanomodified adhesives. Mater Des 2012; 41: 394–402.
10. You M, Yan ZM, Zheng XL, Yu HZ, Li Z. A numerical and experimental study of adhesively bonded aluminium single lap joints with an inner chamfer on the adherends. Int J Adhes Adhes 2008; 28: 71–6.
11. Campilho RDSG, de Moura MFSF, Domingues JJMS. Using a cohesive damage model to predict the tensile behaviour of CFRP single-strap repairs. Int J Solids Struct 2008; 45: 1497–512.
12. Zielecki W., Kubit A., Kluz R., Trzepieciński T. Investigating the influence of the chamfer and fillet on the high-cyclic fatigue strength of adhesive joints of steel parts. 2017; 31(6): 627-644.
13. Belingardi G, Goglio L, Tarditi A. Investigating the effect of spew and chamfer size on the stresses in metal/plastics adhesive joints. Int. J. Adhes. Adhes. 2002; 22: 273–282.
14. You M, Yan Z, Zheng X, Yu H., Li Z. A. A numerical and experimental study of adhesively bonded aluminium single lap joints with an inner chamfer on the adherends. Int. J. Adhes. Adhes. 2007; 28: 71–76.
15. da Silva, L.F.M.; Adams, R.D. Techniques to reduce the peel stresses in adhesive joints with composites. Int. J. Adhes. Adhes. 2007; 27: 227–235.
16. Kaye R, Heller M. Through-thickness shape optimisation of typical double lap-joints including effects of differential thermal contraction during curing. Int J Adhes Adhes 2005; 25: 227.
17. Ashcroft IA, Abdel Wahab MM, Crocombe AD, Hughes DJ, Shaw SJ. The effect of environment on the fatigue of bonded composite joints. Part I: testing and fractography. Compos Part A Appl Sci 2001; 32: 45–58.
18. Chaves FJP, da Silva LFM, de Castro PMST.

Adhesively bonded T-joints in polyvinyl chloride windows. J Mater Des Appl 2008; 222: 159–74.

19. Akpinar, S.; Doru, M.O.; Özel, A.; Aydin, M.D.; Jahanpasand, H.G. The effect of the spew fillet on an adhesively bonded single-lap joint subjected to bending moment. Compos. Part B Eng. 2013; 55: 55–64.
20. Cognard, J.Y.; Creachcadec, R.; Maurice, J. Numerical analysis of the stress distribution in single-lap shear tests under elastic assumption—Application to the optimisation of the mechanical behavior. Int. J. Adhes. Adhes. 2011; 31: 715–724.
21. Hildebrand M. Non-linear analysis and optimisation of adhesively bonded single lap joints between fibre-reinforced plastics and metals. Int J Adhes Adhes Oct. 1994; 14(4): 261–7. https://doi.org/10.1016/0143-7496(94)90039-6.
22. Lang TP, Mallick PK. Effect of spew geometry on stresses in single lap adhesive joints. Int J Adhes Adhes Jun. 1998; 18(3): 167–77. https://doi.org/10.1016/S0143-7496(97)00056-0.
23. Belingardi G, Goglio L, Tarditi A. Investigating the effect of spew and chamfer size on the stresses in metal/plastics adhesive joints. Int J Adhes Adhes Jan. 2002; 22(4): 273–82. https://doi.org/10.1016/S0143-7496(02)00004-0.
24. Hua Y, Gu L, Trogdon M. Three-dimensional modeling of carbon/epoxy to titanium single-lap joints with variable adhesive recess length. Int J Adhes Adhes Oct. 2012; 38: 25–30. https://doi.org/10.1016/j.ijadhadh.2012.06.003.
25. Fessel G, Broughton JG, Fellows NA, Durodola JF, Hutchinson AR. Evaluation of different lap-shear joint geometries for automotive applications. Int JAdhes Adhes 2007; 27: 574–83.
26. Campilho RDSG,Pinto AMG, Banea MD, Silva RF, da Silva LFM, Strength improvement of adhesively-bonded joints using a reverse-bent geometry, J Adhes Sci Technol, in press.
27. Sancaktar E, Simmons SR. Optimization of adhesively-bonded single lap joints by adherend notching. J Adhes Sci Technol 2000; 14: 1363–404.
28. Yan ZM, You M, Yi XS, Zheng XL, Li Z. A numerical study of parallel slot in adherend on the stress distribution in adhesively bonded aluminium single lap joint. Int J Adhes Adhes 2007; 27: 687–95.
29. ISO - ISO 25178-2:2012 - Geometrical product specifications (GPS) — Surface texture: Areal — Part 2: Terms, definitions and surface texture parameters, (n.d.). https://www.iso.org/standard/42785.html (accessed December 28, 2020).
30. W. Macek, R. Branco, P. Podulka, R. Masoudi Nejad, J.D. Costa, J.A.M. Ferreira, C. Capela, The correlation of fractal dimension to fracture surface slope for fatigue crack initiation analysis under bending-torsion loading in high-strength steels, Measurement. 2023; 218: 113169. https://doi.org/10.1016/J.MEASUREMENT.2023.113169.
31. W. Macek, Fractal analysis of the bending-torsion fatigue fracture of aluminium alloy, Eng Fail Anal. 2019; 99: 97–107. https://doi.org/10.1016/j.engfailanal.2019.02.007.
32. Macek W. Correlation between Fractal Dimension and Areal Surface Parameters for Fracture Analysis after Bending-Torsion Fatigue. Metals 2021; 11(11): 1790. https://doi.org/10.3390/met11111790.
33. Macek W., Martins R. F., Branco R., Marciniak Z., Szala M., Wroński S.: Fatigue fracture morphology of AISI H13 steel obtained by additive manufacturing. International Journal of Fracture. 2022; 235: 79–98. https://doi.org/10.1007/s10704-022-00615-5.